Connexin-43 Hemichannels Mediate Cyclic ADP-ribose Generation and Its Ca^{2+}-mobilizing Activity by NAD$^+$/Cyclic ADP-ribose Transport*[S]

Eun-Kyung Song[‡], So-Young Rah[§], Young-Rae Lee[§], Chae-Hwa Yoo[‡], Yu-Ri Kim[‡], Ji-Hyun Yeom[‡], Kwang-Hyun Park[§], Jong-Suk Kim[§], Uh-Hyun Kim[§1], and Myung-Kwan Han[‡¶2]

From the Departments of [‡]Microbiology and [§]Biochemistry and [¶]Institute for Medical Science, Chonbuk National University Medical School and Hospital, Jeonju 561-182, Korea

Background: The ADP-ribosyl cyclase CD38 produces cyclic ADP-ribose from NAD$^+$ in the extracellular space. Cyclic ADP-ribose induces intracellular Ca^{2+} mobilization.

Results: We demonstrate that connexin 43 hemichannels import cyclic ADP-ribose to the intracellular target ryanodine receptor.

Conclusion: Connexin 43 hemichannels mediate the extracellular production and Ca^{2+}-mobilizing action of cyclic ADP-ribose.

Significance: We show that connexin 43 hemichannels resolve the topological hindrance between CD38 and ryanodine receptor.

The ADP-ribosyl cyclase CD38 whose catalytic domain resides in outside of the cell surface produces the second messenger cyclic ADP-ribose (cADPR) from NAD$^+$. cADPR increases intracellular Ca^{2+} through the intracellular ryanodine receptor/Ca^{2+} release channel (RyR). It has been known that intracellular NAD$^+$ approaches ecto-CD38 via its export by connexin (Cx43) hemichannels, a component of gap junctions. However, it is unclear how cADPR extracellularly generated by ecto-CD38 approaches intracellular RyR although CD38 itself or nucleoside transporter has been proposed to import cADPR. Moreover, it has been unknown what physiological stimulation can trigger Cx43-mediated export of NAD$^+$. Here we demonstrate that Cx43 hemichannels, but not CD38, import cADPR to increase intracellular calcium through RyR. We also demonstrate that physiological stimulation such as Fcγ receptor (FcγR) ligation induces calcium mobilization through three sequential steps, Cx43-mediated NAD$^+$ export, CD38-mediated generation of cADPR and Cx43-mediated cADPR import in J774 cells. Protein kinase A (PKA) activation also induced calcium mobilization in the same way as FcγR stimulation. FcγR stimulation-induced calcium mobilization was blocked by PKA inhibition, indicating that PKA is a linker between FcγR stimulation and NAD$^+$/cADPR transport. Cx43 knockdown blocked extracellular cADPR import and extracellular cADPR-induced calcium mobilization in J774 cells. Cx43 overexpression in Cx43-negative cells conferred extracellular cADPR-induced calcium mobilization by the mediation of cADPR import. Our

data suggest that Cx43 has a dual function exporting NAD$^+$ and importing cADPR into the cell to activate intracellular calcium mobilization.

Cyclic ADP-ribose (cADPR)[3] is produced from NAD$^+$ by the ADP-ribosyl cyclase CD38, a type II transmembrane glycoprotein first identified as a lymphocyte differentiation antigen. cADPR directly binds to types II and III ryanodine receptors (RyRs) to induce Ca^{2+} release from RyR containing Ca^{2+} stores located in the sarcoplasmic and endoplasmic reticulum in a variety of cells (1–3). In a limited number of cell systems, cADPR binds to FKBP12.6 and mediates responsiveness of RyR toward cADPR (4–5). The cADPR-mediated increase in intracellular Ca^{2+} concentration ([Ca^{2+}]$_i$) controls various biological processes including egg fertilization (6–7), cell activation, and proliferation (8–9), muscle contraction (10), hormone secretion (11–12), and immune responses (13).

The catalytic site of CD38 is located outside of the cell, but the substrate NAD$^+$ is inside. Moreover, all cADPR targets are located inside and not in direct contact with extracellular cADPR. Therefore, the CD38/cADPR/Ca^{2+} signaling system has two topological questions, the way to export NAD$^+$ to CD38 and the way to import cADPR to its intracellular targets. These topological problems have been described as the topological paradox (14). Many efforts have been done to solve the topological paradox. It has been reported that approach of intracellular NAD$^+$ to ecto-CD38 could be carried out by connexin 43 (Cx43) hemichannels, a component of gap junctions (15), and that approach of cADPR to its intracellular target

[S] The on-line version of this article (available at http://www.jbc.org) contains supplemental Figs. S1 and S2.

[1] To whom correspondence may be addressed. Tel.: (+82)-63-270-3083; Fax: (+82)-63-274-9833; E-mail: uhkim@chonbuk.ac.kr.

[2] To whom correspondence may be addressed: Tel.: (+82)-63-270-3106; Fax: (+82)-63-274-9833; E-mail: iamtom@chonbuk.ac.kr.

[3] The abbreviations used are: cADPR, cyclic ADP-ribose; RyR, ryanodine receptors; [Ca^{2+}]$_i$, intracellular Ca^{2+} concentration; Cx43, connexin 43; FcγR, Fcγ receptor; HBSS, Hank's balanced salt solution; IP$_3$, inositol trisphosphate; PKA, protein kinase A; MAPK, mitogen-activated protein kinase; PKC, protein kinase C; JNK, c-Jun N-terminal kinase.

could be carried out by CD38 oligomer and nucleoside transporters (16–17). However, it still remains unclear whether the import of cADPR by CD38 oligomer and nucleoside transporters is involved in cADPR/Ca^{2+} signaling in response to physiological stimulation.

In this study we demonstrate that Cx43 hemichannels act as a dual nucleotide transporter for NAD^+ export/cADPR import and link ectocellular production of cADPR by CD38 and intracellular action of cADPR by RyR. We also demonstrate that physiological stimulation such as Fcγ receptor (FcγR) ligation triggers intracellular Ca^{2+} mobilization using Cx43-mediated NAD^+ export/cADPR import system.

EXPERIMENTAL PROCEDURES

Cell Culture—The J774A.1 murine macrophage cell line was obtained from American Type Culture Collection and cultured at 37 °C in Dulbecco's Modified Eagle's Media (DMEM, Invitrogen) supplemented with 10% heat-inactivated and sterile-filtered fetal bovine serum (FBS), 2 mM glutamine, 100 units/ml penicillin, and 100 μg/ml streptomycin. The cells were passaged twice a week, and cells older than 15 passages were not used. Resident peritoneal cells were isolated from C57BL/126 mice 8 to 12 weeks of age, purified with a ficoll density gradient as described (18), and cultured at 37 °C in the J774 cell culture medium.

Phagocytic Assay—J774A.1 cells were plated at a density of 1×10^5 cells per well in a 12-well plate (Corning Costar) and cultured overnight. For phagocytosis, the medium was exchanged with DMEM containing IgG-coated sheep red blood cells (IgG-SRBC) for 30 min. IgG-SRBC was prepared by incubating SRBC with 1:10 dilution of the maximal subagglutinating titer of rabbit anti-SRBC IgG (ICN-Cappel). Cell surface-bound SRBC were lysed with hypotonic buffer, and the cells were fixed in 3.7% paraformaldehyde. Phagocytosis was assessed by counting SRBC in J774 cells on a light microscope. The phagocytic index was calculated as follows: phagocytic index (PI) = number of SRBCs internalized by 100 J774 cells counted in 10 random fields.

Preparation of IgG Complex—Bovine serum albumin (BSA) (Sigma-Aldrich) and rabbit anti-BSA IgG antibody (Sigma-Aldrich) were mixed in an antigen/antibody ratio of 1:1 (wt/wt) after removing endotoxin by passage through endotoxin-removing gel (Thermo Fisher Scientific). The reaction mixture was incubated at 37 °C for 1 h and thereafter at 4 °C overnight. The formed immunoprecipitates were centrifuged at 10,000 rpm for 10 min at 4 °C, and soluble immune complex in the supernatant was obtained.

$[Ca^{2+}]_i$ Measurements—$[Ca^{2+}]_i$ in J774A.1 cells, peritoneal macrophages and ZR70-1 cells were measured using a confocal microscope (Nikon, Japan) as described previously (19). The cells were cultured on 100 μg/ml poly L-lysine-coated confocal dishes for 3 h, washed with Hank's balanced salt solution (HBSS) (2 mM $CaCl_2$, 145 mM NaCl, 5 mM KCl, 1 mM $MgCl_2$, 5 mM D-glucose, and 20 mM HEPES, pH 7.4) and then loaded with 5 μM Fluo3 AM (Molecular Probes, Eugene, OR) for 1 h. Sulfinpyrazone (250 μM) was added to prevent dye leakage. Changes in Ca^{2+} fluorescence were measured at 488 nm/530 nm (excitation/emission) by an air-cooled argon laser system. $[Ca^{2+}]_i$ in

HEK293 cells were determined by using a PTI fluorometer (Photon Technology International). HEK293 cells were incubated with 4 μM Fura-2 AM in RPMI 1640 medium containing 3% fetal bovine serum for 60 min at 37 °C. Fura-2-loaded cells were then washed twice with HBSS. For fluorometric measurement of Ca^{2+}, 5×10^6 cells were placed in a quartz cuvette in a thermostatically controlled cell holder at 37 °C, and the cell suspension was stirred continuously. Fluorescence ratios were taken with an alternative wavelength time scanning method (dual excitation at 340 and 380 nm; emission at 510 nm). $[Ca^{2+}]_i$ was calculated by the method of Tsien *et al.* (20). For the calculation of $[Ca^{2+}]_i$, the method of Tsien *et al.* (20) was used with the following equation: $[Ca^{2+}]_i = K_d (F - F_{min})/(F_{max} - F)$, where K_d is 325 nM and 342 nM for Fluo-3 and Fura 2, respectively, and F is the observed fluorescence levels. Each tracing was calibrated for the maximal intensity (F_{max}) by the addition of ionomycin (8 μM) and for the minimal intensity (F_{min}) by the addition of EGTA (50 mM) at the end of each measurement.

Knockdown of CD38 and Cx43 Using siRNAs—We purchased control and CD38 siRNAs from Santa Cruz Biotechnology. We purchased control and Cx43 siRNA from Dharmacon RNAi Technologies. A total of 60 pmol of siRNA duplexes were transfected into 0.5×10^6 cells using Nucleofector (Amaxa Inc., Gaithersburg, MD) and cultured for 48 h. Knockdown of CD38 and Cx43 was confirmed by Western blotting using anti-CD38 and anti-Cx43 antibody, respectively (Santa Cruz).

Preparation of [Adenine-2,8-³H]cADPR from [Adenine-2,8-³H]NAD⁺—300 μM [Adenine-2,8-³H]NAD⁺ ([adenine-2,8-³H]NAD⁺:cold NAD⁺ = 1:100) was incubated with 1 μg ADP-ribosyl cyclase at 4 °C for 1 h. cADPR was purified by AG MP-1 ion exchange columns. The reaction mixture was injected into the AG-MP-1 column and eluted by a gradient from water (eluent A) to 150 mM trifluoroacetic acid (eluent B) at a flow rate of 4 ml/min. The gradient was (in % of eluent B): 0 min, 0%; 6 min, 0%; 11 min, 4%; 16 min, 8%; 18 min, 11.6%; 20 min, 100%; 24 min, 100%; 26 min, 0%; 30 min, 0%. Absorbance was measured at 254 nm, and the eluting fraction following 11–13 min was collected and lyophilized.

Uptake of [Adenine-2,8-³H]cADPR by J774 Cells—The uptake of [adenine-2,8-³H]cADPR was measured by a rapid oil-stop method (21) with some modifications. The reaction was initiated by addition of 5 μl of 100 μM [adenine-2,8-³H]cADPR to 45 μl of 1×10^6 J774 cell suspension on a 50 μl oil layer (silicone oil/paraffin oil, 80:20) and ended by pelleting the cells into the oil layer at 15,000 $\times$ g for 30 s. The tubes were frozen and cut through the oil layer, and the radioactivity associated with the cells was measured by liquid scintillation counting.

Confocal Microscopy—J774A.1 cells were cultured on gelatin-coated glass coverslips for 24 h. The cells were washed three times with phosphate buffered saline (PBS), and fixed for 20 min with 3% paraformaldehyde in PBS. The fixed cells were then washed three times with PBS and incubated with 50 mM NH_4Cl for 10 min to quench the crosslinking reaction. The cells were further washed three times with PBS and then treated with blocking buffer (10% FBS in PBS) for 30 min at room temperature. The nonspecific binding of immunoglobulins to the mouse Fcγ receptors was blocked by incubation with anti-mouse CD16/CD32 receptor monoclonal antibody at 1 μg/100

μl (Pharmingen). CD38 in the cells was stained with anti-mouse CD38 (eBiosciences) and Alexa Fluor® 647 goat anti-mouse IgG antibodies (Santa Cruz Biotechnology), followed by washing in PBS. Cx43 in the cells were then stained with anti-mouse Cx43 (Santa Cruz Biotechnology) and Alexa Fluor® 488 goat anti-rabbit IgG antibodies (Invitrogen), followed by washing in PBS. The coverslips were then washed extensively in PBS and mounted using a vectashield medium (Vector Laboratories). Specimens were viewed using a Zeiss laser scanning confocal microscope.

Coimmunoprecipitation and Western Blotting—For coimmunoprecipitation studies, cell pellets derived from 1×10^7 J774 cells were lysed in coimmunoprecipitation buffer (50 mM Tris, pH 7.5, 150 mM NaCl, 1% Nonidet P-40, 1 mM EDTA, 1% glycerol, 1 mM dithiothreitol, and protease inhibitors). The homogenates were centrifuged for 20 min at $14,000 \times g$ at 4 °C, and the supernatants were precleared with Preclearing matrix A-mouse (Santa Cruz) for CD38 immunoprecipitation or Preclearing matrix A-rabbit (Santa Cruz) for Cx43 immunoprecipitation and combined with 20 μl (packed gel) of either anti-CD38 or anti-Cx43 IP matrix. To prepare anti-CD38 and anti-Cx43 IP matrix, 50 μl of IP matrix (Santa Cruz) are mixed with 2 μg of anti-CD38 (eBioscience) and anti-Cx43 (Santa Cruz) antibodies, respectively and mixed overnight at 4 °C. The precipitates were washed twice in high-salt buffer (coimmunoprecipitation buffer with 500 mM NaCl, 0.1% Nonidet P-40) and twice in low-salt buffer (coimmunoprecipitation buffer with 0.1% Nonidet P-40, but no NaCl). CD38 and Cx43 precipitates were separated by SDS-PAGE on a 12% polyacrylamide gel and transferred to a PVDF membrane. The membrane was blocked with 2% bovine serum albumin and probed with antibodies against CD38 and Cx43 (Santa Cruz Biotechnology). The membrane was then incubated with goat Exactacruz™ A-HRP (Santa Cruz Biotechnology) and developed with enhanced chemiluminescence PLUS reagent from Amersham Biosciences (Piscataway, NJ).

Ectopic Expression of Cx43 and/or RyR1—The RyR1 expression vector pcDNA3-RyR1 was kindly provided by Professor P. D. Allen (Brigham and Women's Hospital). The Cx43 expression vector pCMV-SPORT6-connexin43 was purchased from Invitrogen. HEK293 cells were transfected, in 100-cm² plasticware, with 5 μg of pcDNA-RyR1 and/or pCMV-SPORT6-connexin43 using Lipofectamine (Invitrogen) according to the manufacturer's instructions. Cx43-overexpressing lentiviral vector was constructed by a gateway cloning system using pCMV-SPORT6-connexin43, pDONR223, and pLenti6/V5-DEST gateway vector kit (Invitrogen). Cx43-overexpressing lentiviral particles were generated by transfection of 293T with Cx43-overexpressing lentiviral vector. Jurkat cells were infected with Cx43-overexpressing lentiviral particles and selected with blasticidin.

Extracellular NAD⁺ Determination—To measure the concentration of extracellular NAD^+, the cycling assay for NAD^+ was applied with a little modification. The extracellular supernatant was added to an equal volume of reaction mixture that contained 2% ethanol, 0.1 mg/ml BSA, 10 μM FMN, 10 μg/ml diaphorase, 20 μM resazurin, 100 μg/ml alcohol dehydrogenase. It was allowed to incubate for 2 h at room temperature. The

fluorescence increase of resorufin was measured by Hitachi fluorometry (ex. 544 nm, em. 590 nm).

Statistical Analysis—All results are presented as the mean and standard error of at least three independent experiments. Statistical significance was calculated by Student"s *t* test using the Sigmaplot software.

RESULTS

FcγR Stimulation-induced Ca^{2+} Increase Is Dependent on CD38 and Cx43 Expression in J774 Cells—We previously demonstrated that CD38 is expressed in J774 cells and is involved in the regulation of FcγR-mediated phagocytosis (22). In the present study we first analyzed whether FcγR stimulation induces Ca^{2+} increase and if CD38 is involved in the signaling. FcγR stimulation with an IgG complex induced a Ca^{2+} transient in J774 cells (Fig. 1A). CD38 knockdown blocked FcγR stimulation-induced Ca^{2+} increase (Fig. 1A). Moreover, 8-bromo-cADPR, a cADPR antagonist, blocked FcγR stimulation-induced Ca^{2+} increase but not xestospongin, an inositol trisphosphate (IP_3) antagonist (Fig. 1B). These data indicate that CD38 mediates FcγR stimulation-induced Ca^{2+} increase through cADPR production. We next examined whether Cx43 hemichannels are involved in CD38-mediated Ca^{2+} signaling upon FcγR stimulation since Cx43 hemichannels have been suggested to transport intracellular NAD^+ to CD38 (15). Cx43 knockdown also completely abolished FcγR stimulation-induced $[Ca^{2+}]_i$ increase (Fig. 1C). CD38 and Cx43 were primarily colocalized in the plasma membrane of J774 cells by double immunofluorescent staining (Fig. 1D). Further evidence that CD38 and Cx43 interact in the membrane was obtained from co-immunoprecipitation analyses, using extracts from J774 cells. Immunoprecipitation of J774 cell lysates with anti-CD38 recovered a protein that was reactive to anti-Cx43 antibody and *vice versa* (Fig. 1E). These data show that FcγR stimulation activates a signaling pathway involving CD38 and Cx43, and induces a Ca^{2+} increase.

FcγR Stimulation Exports NAD^+ through Cx43 Hemichannels in J774 Cells—We next examined whether Cx43 hemichannels export NAD^+ to CD38 upon FcγR stimulation. FcγR stimulation with an IgG complex exported NAD^+ in a time-dependent manner (Fig. 2A). Cx43 knockdown inhibited FcγR stimulation-induced NAD^+ export by 80% (Fig. 2B). Moreover, degradation of extracellular NAD^+ by the treatment of Neurospora NADase abolished FcγR stimulation-induced $[Ca^{2+}]_i$ increase (Fig. 2C). These data suggest that FcγR stimulation triggers Cx43-mediated NAD^+ export and initiates CD38/cADPR/Ca^{2+} signaling. This is the first evidence showing that Cx43-mediated NAD^+ export is activated by a physiological ligand.

Cx43 Hemichannels Import cADPR as Well as Export NAD^+—To clearly confirm that NAD^+ exported by Cx43 hemichannels can participate in NAD^+/CD38/cADPR/Ca^{2+} signaling, we tested whether exogenous NAD^+ increases $[Ca^{2+}]_i$ through its conversion by CD38 into cADPR. The exogenous NAD^+ triggered a Ca^{2+} increase in a similar pattern to FcγR stimulation-induced Ca^{2+} increase (Fig. 3A, *left*). The exogenous NAD^+-triggered Ca^{2+} increase was blocked by 8-bromo-cADPR (Fig. 3A, *right*), indicating the exogenous NAD^+-triggered Ca^{2+}
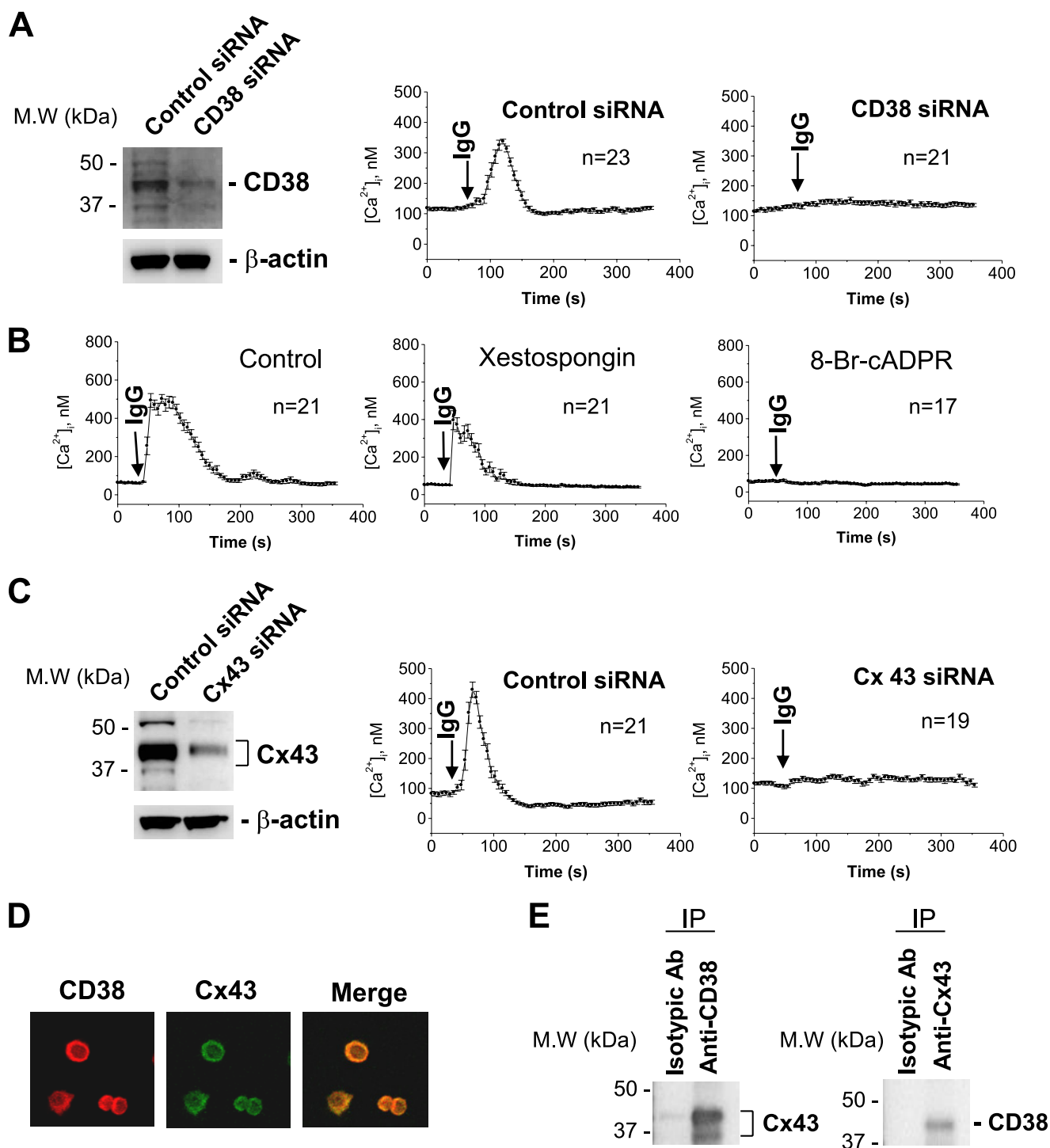
FIGURE 1. **FcγR stimulation-induced [Ca^{2+}]$_i$ increase is dependent on CD38 and Cx43 expression.** *A*, effect of CD38 on FcγR stimulation-induced [Ca^{2+}]$_i$ increase. J774 cells were transfected with control or CD38 siRNA. 48-h later, we analyzed expression levels of CD38 by Western blot and measured [Ca^{2+}]$_i$ using a confocal microscope after addition of IgG complex to Fluo-3/AM-loaded J774 cells. *B*, effect of xestospongin and 8-bromo-cADPR on FcγR stimulation-induced [Ca^{2+}]$_i$ increase in J774 cells. IgG complex (100 μg/ml) was added to Fluo-3/AM-loaded J774 cells that were preincubated with 2 μM xestospongin or 50 μM 8-bromo-cADPR for 30 min. [Ca^{2+}]$_i$ changes were measured using a confocal microscope. *C*, effect of Cx43 knockdown on FcγR stimulation-induced [Ca^{2+}]$_i$ increase. J774 cells were transfected with control or connexin 43 siRNA. 48 h later, we analyzed expression levels of Cx43 by Western blot and measured [Ca^{2+}]$_i$ changes in Fluo-3/AM-loaded J774 cells using a confocal microscope. *D*, colocalization of CD38 and Cx43 in J774 cells (CD38 in *red* and Cx43 in *green*, with a merged image). Double immunolabeling of J774 cells was carried out by staining with either anti-CD38 or Cx43 antibody. Primary antibodies were visualized with fluorescein isothiocyanate-labeled anti-mouse IgG or rhodamine isothiocyanate labeled anti-rabbit IgG. *E*, coimmunoprecipitation between Cx43 and CD38. J774 cell lysates were immunoprecipitated with anti-CD38 and anti-Cx43 antibody. Cx43 was detected in immunoprecipitates with anti-CD38 (*left panel*), and CD38 was detected in immunoprecipitates with anti-Cx43 (*right panel*). Each *line* represents mean ± S.E. of [Ca^{2+}]$_i$ (*A–C*).

increase is through cADPR production. This was further confirmed by the finding that blocking NAD$^+$ conversion into cADPR by CD38 knockdown abolished the exogenous NAD$^+$-triggered Ca^{2+} increase (Fig. 3B, *center*). Unexpectedly, Cx43 knockdown abolished the exogenous NAD$^+$-triggered Ca^{2+} increase (Fig. 3B, *right*). In addition, Cx43 knockdown abol-

A

B

C
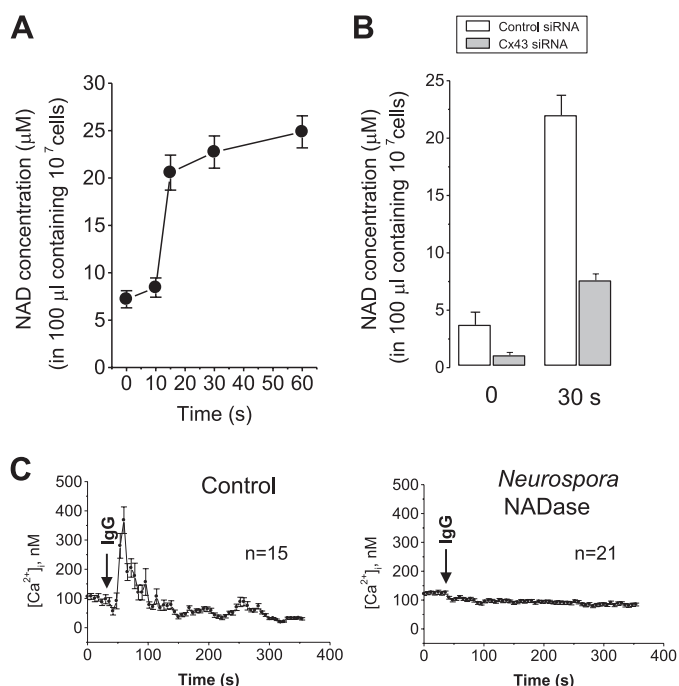
FIGURE 2. **The requirement of Cx43-mediated NAD$^+$ secretion in FcγR stimulation-induced [Ca^{2+}]$_i$ increase.** *A*, NAD$^+$ secretion by FcγR stimulation. J774 cells were treated with an IgG complex for the indicated time. After centrifugation, NAD$^+$ in the supernatant was determined. The data represent mean ± S.E.. *B*, effect of Cx43 knockdown on FcγR stimulation-induced NAD$^+$ secretion. J774 cells were transfected with control or connexin 43 siRNA. 48 h later, J774 cells were treated with an IgG complex for 30 s. After centrifugation, NAD$^+$ in the supernatant was determined. The data represent mean ± S.E. *C*, effect of NADase on FcγR stimulation-induced [Ca^{2+}]$_i$ increase. Fluo-3 AM-loaded J774 cells were pretreated with 1 μg/ml *Neurospora crassa* NADase. Ten min later, IgG complex was added to the cells, and [Ca^{2+}]$_i$ changes were measured using a confocal microscope. Each *line* represents mean ± S.E. of [Ca^{2+}]$_i$.

ished the exogenous cADPR-triggered Ca^{2+} increase but CD38 knockdown didn't (Fig. 3*C*). Epidermal growth factor, a CD38-independent stimulus, triggered Ca^{2+} increase in Cx43 knockdown cells as well as control cells (supplemental Fig. S1), indicating that Cx43 knockdown had no effect on other Ca^{2+} signaling systems. Cx43 hemichannel blockers such as 18β-glycyrrhetinic acid, La^{3+}, octanol, and oleamide inhibited the exogenous cADPR-triggered Ca^{2+} increase (supplemental Fig. S2). These findings suggest that Cx43 hemichannels are involved in the access of cADPR to its intracellular target site. To examine whether Cx43 hemichannels import cADPR, we measured cADPR uptake using [^{3}H]cADPR and analyzed the effect of Cx43 knockdown on cADPR uptake. cADPR uptake was increased in a time-dependent manner (Fig. 3*D*). cADPR uptake was blocked by Cx43 knockdown by ~80% but not by CD38 knockdown (Fig. 3*E*). Taken together, our data indicate that Cx43 hemichannels are an essential partner of CD38 in cADPR-mediated Ca^{2+} signaling through the export of the CD38 substrate NAD$^+$ and import of the CD38 product cADPR.

Ectopic Expression of Cx43 Confers Exogenous cADPR-induced Increase in [Ca^{2+}]$_i$ to Cx43-negative Cells—To further confirm the role of Cx43 hemichannels as a cADPR importer, we infected Cx43-negative Jurkat cells with Cx43-expressing lentivirus and measured cADPR uptake and exogenous

cADPR-induced increase in [Ca^{2+}]$_i$. Cx43 overexpression increased cADPR uptake (Fig. 4, *A* and *B*). cADPR did not induce any [Ca^{2+}]$_i$ increase in control lentivirus-infected Jurkat cells (Fig. 4*C*). Cx43 overexpression showed a cADPR-induced [Ca^{2+}]$_i$ increase (Fig. 4*C*). We also transfected Cx43 and RyR genes in HEK293 cells and analyzed exogenous cADPR-induced increase in [Ca^{2+}]$_i$ (Fig. 4, *D--F*). HEK293 cells were unresponsive to extracellular cADPR (Fig. 4*E*). Despite Cx43 overexpression by transfection of the Cx43 gene, HEK293 cells were still unresponsive to exogenous cADPR (Fig. 4*E*). However, transfection of the RyR gene confers an exogenous cADPR-induced increase in [Ca^{2+}]$_i$ to HEK293 cells (Fig. 4, *E* and *F*). Co-transfection of Cx43 and RyR genes in HEK 293 cells further increased [Ca^{2+}]$_i$ compared with either Cx43 or RyR transfection alone (Fig. 4, *E* and *F*). These data indicate that expression of both Cx43 and RyR is required for the extracellular cADPR-induced [Ca^{2+}]$_i$ increase. These data confirm that Cx43 hemichannels are an importer of cADPR.

Protein Kinase A (PKA) Activates Cx43/CD38/cADPR/Ca^{2+}-signaling Pathway—Our next goal was to determine what activates the Cx43/CD38/cADPR/Ca^{2+} signaling pathway. In this study, we showed that FcγR stimulation activates the Cx43/CD38/cADPR/Ca^{2+} signaling pathway (Fig. 1). This finding suggests that FcγR downstream activates the pathway. To confirm this hypothesis, we used several inhibitors of signal transduction including inhibitors of PKA (H89), protein kinase C (PKC) (AEB071), phosphatase (okadaic acid), p 38 mitogen-activated protein kinase (MAPK) (SB203580), c-Jun N-terminal kinase (JNK) (SP600125), and extracellular signal-regulated kinase (ERK) (PD098059), and analyzed the effects of these inhibitors on FcγR stimulation-, extracellular NAD$^+$-, or cADPR-induced [Ca^{2+}]$_i$ increases. H89 and SP600125, but not the other inhibitors, significantly inhibited the FcγR stimulation-induced [Ca^{2+}]$_i$ increase (Fig. 5*A*). H89 inhibited only the FcγR stimulation-induced [Ca^{2+}]$_i$ increase, but SP600125 inhibited extracellular NAD$^+$-, cADPR-, and FcγR stimulation-induced [Ca^{2+}]$_i$ increases (Fig. 5*B*). This suggests that H89 inhibits NAD$^+$ secretion induced by FcγR stimulation without affecting Cx43-mediated import of cADPR. Indeed, H89 inhibited FcγR stimulation-induced secretion of NAD$^+$, but SP600125 did not (Fig. 5*C*), indicating that PKA acts upstream of the CD38/cADPR-signaling pathway, and JNK acts downstream of cADPR. To test whether PKA directly activates the Cx43/CD38/cADPR/Ca^{2+}-signaling pathway, we analyzed the effects of forskolin, a PKA activator. Forskolin induced a Ca^{2+} increase that was blocked by the treatment of 8-bromo-cADPR and the knockdown of CD38 or Cx43 in J774 cells (Fig. 6, *A* and *B*). Forskolin also increased NAD$^+$ secretion (Fig. 6*C*). *Neurospora* NADase, an NAD$^+$-degrading enzyme without cADPR production, abrogated the forskolin-induced [Ca^{2+}]$_i$ increase (Fig. 6*D*), indicating that PKA activation-induced NAD$^+$ secretion initiates the Cx43/CD38/cADPR/Ca^{2+}-signaling system. We next tested whether PKA mediates NAD$^+$ secretion by Cx43 phosphorylation. FcγR stimulation increased phosphorylation of Cx43, reaching a maximum at 20 s and then decreasing rapidly (Fig. 6*E*). FcγR stimulation-induced Cx43 phosphorylation was completely blocked by H89 (Fig. 6*F*). It is still unclear whether FcγR stimulation-induced Cx43 phosphory-
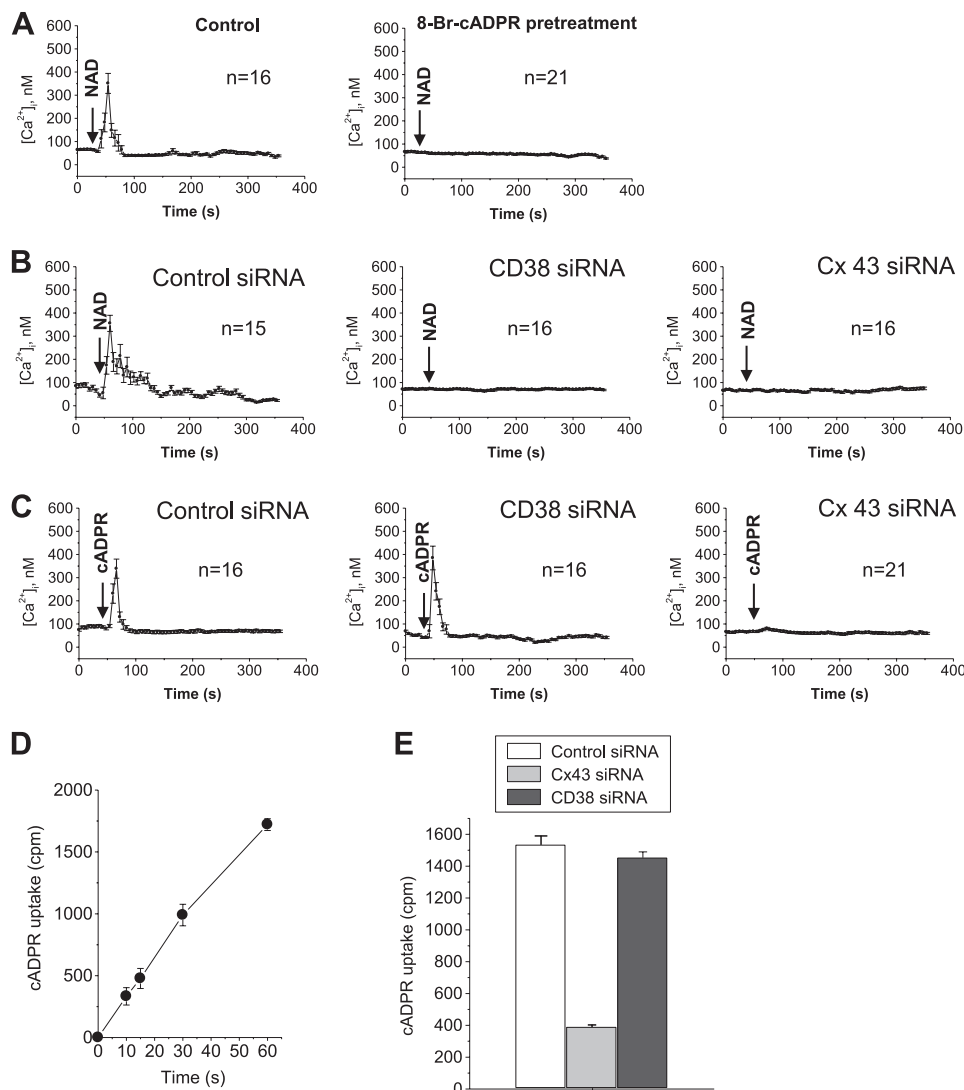
FIGURE 3. **Cx43 hemichannels are a cADPR transporter.** *A*, extracellular NAD^+ increases $[Ca^{2+}]_i$ via cADPR conversion. 100 μM NAD^+ was added to Fluo-3/AM-loaded J774 cells that were preincubated with or without 8-bromo-cADPR for 30 min. $[Ca^{2+}]_i$ changes were measured using a confocal microscope. Each *line* represents mean ± S.E. of $[Ca^{2+}]_i$. *B*, effect of CD38 or Cx43 knockdown on extracellular NAD^+-induced $[Ca^{2+}]_i$ increase. J774 cells were transfected with control, CD38, or Cx43 siRNA and incubated for 48 h. 100 μM NAD^+ was added to Fluo-3/AM-loaded J774 cells and $[Ca^{2+}]_i$ changes were measured using a confocal microscope. Each *line* represents mean ± S.E. of $[Ca^{2+}]_i$. *C*, effect of CD38 or Cx43 knockdown on extracellular cADPR-induced $[Ca^{2+}]_i$ increase. J774 cells were transfected with control, CD38, or Cx43 siRNA and incubated for 48 h. 100 μM cADPR was added to Fluo-3/AM-loaded J774 cells, and $[Ca^{2+}]_i$ changes were measured using a confocal microscope. Each *line* represents mean ± S.E. of $[Ca^{2+}]_i$. *D*, time-dependent uptake of cADPR in J774 cells. J774 cells were incubated with [³H]cADPR for the indicated time. [³H]cADPR uptake was measured. *E*, effect of Cx43 and CD38 knockdown on cADPR uptake in J774 cells. J774 cells were transfected with control, connexin 43, or CD38 siRNA and incubated for 48 h. The cells were incubated with [³H]cADPR for 1 min and [³H]cADPR uptake was measured. The data represent mean ± S.E. Each *line* represents mean ± S.E. of $[Ca^{2+}]_i$ (*A–C*). The data represent mean ± S.E. (*D* and *E*).

lation is related to Cx43-mediated NAD^+ import/cADPR export. The identification of the phosphorylation site and site directed mutagenesis of it is required to demonstrate the relationship. Taken together, PKA is a regulator of the Cx43/CD38/cADPR/Ca^{2+} signaling system and is a linker to the signaling pathway activated by a physiological stimulus such as FcγR stimulation.

CD38 was reported to undergo internalization through non clathrin-coated endocytic vesicles upon exposure to NAD^+, thiol compounds, or agonistic antibodies (12, 23). In the reports, it has been proposed that the effect of CD38-internalizing ligands on intracellular Ca^{2+} levels was suggested to involve a three-step mechanism: 1) export of cytosolic NAD^+ into the endocytotic vesicles, 2) intravesicular CD38-catalyzed

conversion of NAD^+ to cADPR, 3) import of the cyclic nucleotide into the cytosol and subsequent release of Ca^{2+} from RyR stores. It has been reported that export of intracellular NAD^+ to ecto-CD38 could be carried out by Cx43 hemichannels (15), and that import of cADPR to its intracellular target could be carried out by CD38 oligomer and nucleoside transporters (16–17). Here we demonstrated that Cx43 hemichannels export NAD^+ to extracellular space in response to a physiological stimulus, FcγR stimulation, and then extracellular NAD^+ is converted to cADPR by ecto-CD38 that is imported into cytosol through Cx43 hemichannels, thereby resulting in $[Ca^{2+}]_i$ increase. Moreover, we demonstrated that FcγR stimulation induces Cx43-mediated export of NAD^+ via PKA signaling pathway.
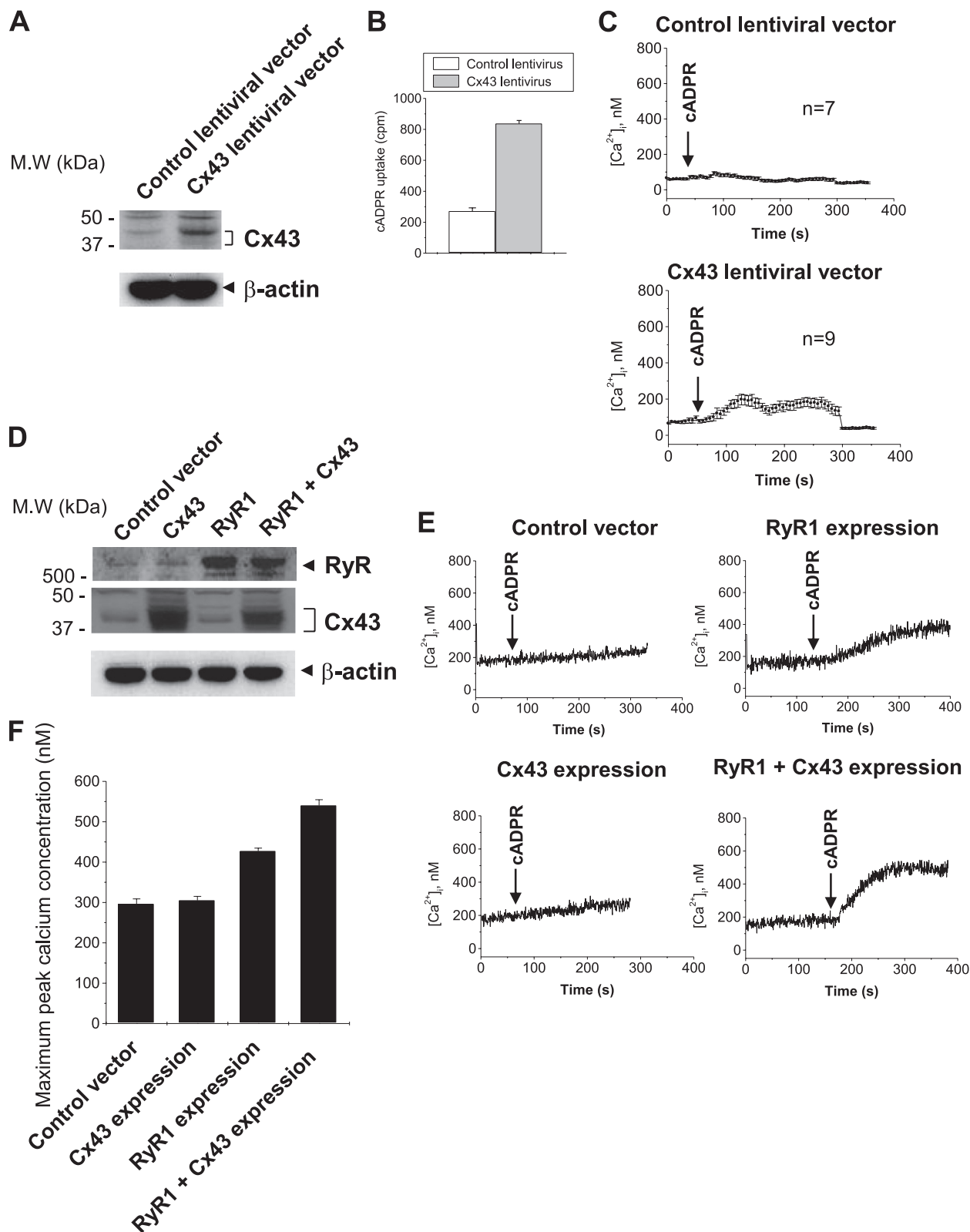
FIGURE 4. **Cx43 overexpression induces extracellular cADPR-induced [Ca^{2+}]$_i$ increase in Jurkat and HEK 293 cells.** *A*, Cx43 overexpression with Cx43-expressing lentivirus in Jurkat cells. Jurkat cells were infected with control or Cx43 expressing lentivirus and selected with blastidin. Cx43 expression level was analyzed by Western blot. *B*, effect of Cx43 overexpression on cADPR uptake in Jurkat cells. Jurkat cells were incubated with [^{3}H]cADPR for 1 min. [^{3}H]cADPR uptake was measured. *C*, effect of Cx43 overexpression on extracellular cADPR-induced [Ca^{2+}]$_i$ increase in Jurkat cells. cADPR was added to Fluo-3/AM-loaded Jurkat cells and [Ca^{2+}]$_i$ changes were measured using a confocal microscope. Each *line* represents mean $\pm$ S.E. of [Ca^{2+}]$_i$ (*D*) Cx43 and RyR overexpression. HEK293 cells were transfected with control, Cx43 and/or RyR expressing vector. Cx43 expression level was analyzed by Western blot. *E*, effect of Cx43 and RyR overexpression on extracellular cADPR-induced [Ca^{2+}]$_i$ increase in HEK 293 cells. cADPR was added to Fura-2/AM-loaded HEK293 cells and [Ca^{2+}]$_i$ changes were measured using a PTI spectrofluorometer. *F*, effect of Cx43 and RyR overexpression on maximum peak Ca^{2+} concentration. [Ca^{2+}]$_i$ changes were measured as described above. The data represent mean $\pm$ S.E. (*B* and *F*).
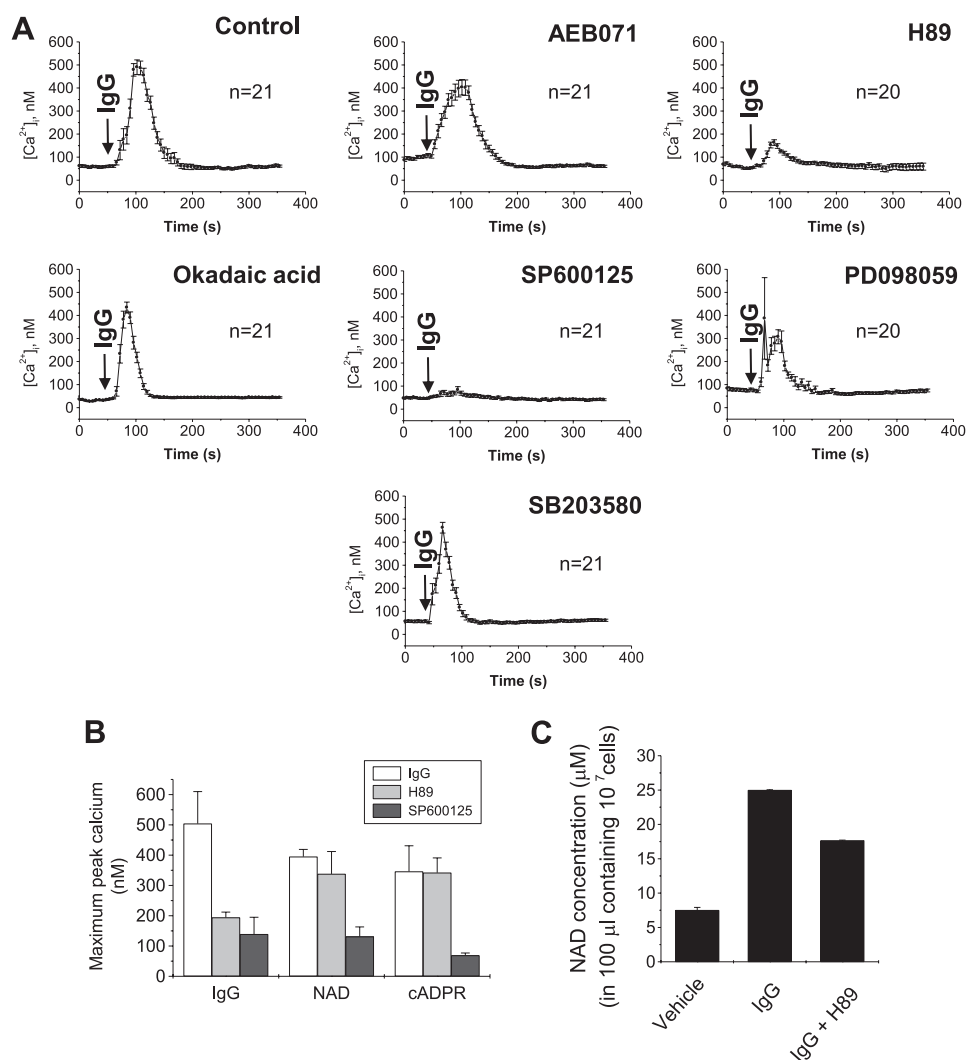
FIGURE 5. **The effect of inhibitors for signal transduction on FcγR stimulation, extracellular NAD$^+$ or cADPR-induced [Ca^{2+}]$_i$ increase.** *A*, effect of inhibitors for signal transduction on FcγR stimulation-induced [Ca^{2+}]$_i$ increase. IgG complex was added to Fluo-3/AM-loaded J774 cells that were pretreated with 1 μM AEB071, 100 nM H89, 5 μM okadaic acid, 5 μM SP600125, 5 μM PD098059, or 10 μM SB203580 for 10 min. [Ca^{2+}]$_i$ changes were measured using a confocal microscope. Each *line* represents mean ± S.E. of [Ca^{2+}]$_i$. *B*. effect of 100 nM H89 and 5 μM SP600125 on FcγR stimulation, extracellular NAD$^+$ or cADPR-induced [Ca^{2+}]$_i$ increase. IgG complex, NAD$^+$ or cADPR was added to Fluo-3/AM-loaded J774 cells that were pretreated with H89 or SP600125 for 10 min. [Ca^{2+}]$_i$ changes were measured using a confocal microscope. The data represent mean ± S.E. of maximum peak [Ca^{2+}]$_i$. *C*, effect of H89 on FcγR stimulation-induced NAD$^+$ secretion. J774 cells were pretreated with 100 nM H89 for 10 min and then treated with IgG complex for 1 min. After centrifugation, NAD$^+$ in the supernatant was determined. The data represent mean ± S.E.

Taken together, we proposed a model for FcγR stimulation-induced [Ca^{2+}]$_i$ increase via Cx43/CD38/cADPR signaling pathway (Fig. 7): FcγR stimulation activates PKA, which causes Cx43 phosphorylation. Cx43 phosphorylation induces NAD$^+$ secretion into extracellular space or endocytic vescles. NAD$^+$ is converted into cADPR which is imported into cytosol via Cx43 hemichannels and increases [Ca^{2+}]$_i$ via RyR. Our data are the first evidence that Cx43-mediated NAD$^+$ secretion responds to physiological ligand activation and is involved in CD38 signaling. We also identified a new function of Cx43 hemichannels as a transporter of cADPR, a general Ca^{2+} mobilizer. Our results suggest that Cx43 hemichannels are a linker of extracellular cADPR generation and its intracellular action.

DISSCUSSION

It has been previously reported that Cx43 hemichannels export NAD$^+$ to extracellular space. However, it has been still unclear whether the function of Cx43 hemichannels to export NAD$^+$ is involved in CD38/cADPR signaling pathway. Here we demonstrated that Cx43-mediated NAD$^+$ secretion is required for CD38/cADPR/Ca^{2+} signaling activated by FcγR stimulation. Our data are the first evidence that Cx43-mediated NAD$^+$ secretion responds to physiological ligand activation and is involved in CD38 signaling.

It has been long questioned how extracellularly generated cADPR is influxed into its intracellular target. Oligomeric CD38 has been regarded as a cADPR importer. It has been reported that oligomeric CD38 transports cADPR in resealed erythrocyte ghosts and artificial membrane (16). However, it has not been demonstrated that oligomeric CD38 can transport cADPR in whole, isolated cells. We found that CD38 knockdown didn't affect extracellular cADPR-induced [Ca^{2+}]$_i$ increase in J774 cells (Fig. 3*C*, *center*). Cx43 knockdown inhibited cADPR uptake but CD38
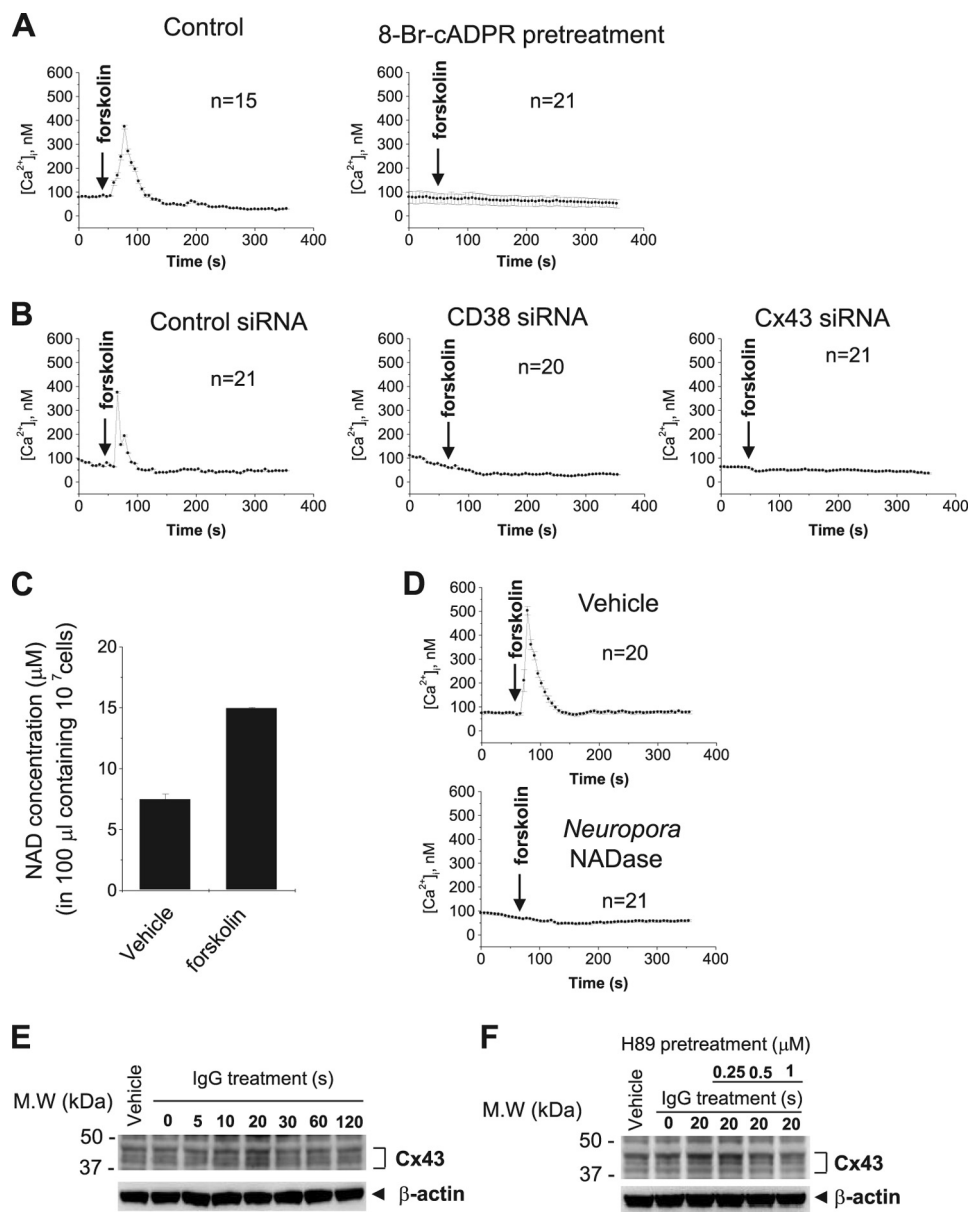
FIGURE 6. **PKA activation activates CD38/cADPR/Ca^{2+} signaling.** *A*, forskolin, a PKA activator, induces [Ca^{2+}]$_i$ increase via cADPR formation. Forskolin was added to Fluo-3/AM-loaded J774 cells that were preincubated with or without 8-bromo-cADPR for 30 min. [Ca^{2+}]$_i$ changes were measured using a confocal microscope. *B*, effect of CD38 and Cx43 knockdown on forskolin-induced [Ca^{2+}]$_i$ increase. J774 cells were transfected with control, CD38 or Cx43 siRNA and incubated with 48 h. After Fluo-3/AM loading, 50 μM forskolin was added and [Ca^{2+}]$_i$ changes were measured using a confocal microscope. *C*, NAD$^+$ secretion by forskolin. J774 cells were treated with 50 μM forkolin for 1 min. After centrifugation, NAD$^+$ in the supernatant was determined. The data represent mean $\pm$ S.E. *D*, effect of NADase on forskolin-induced [Ca^{2+}]$_i$ increase. Fluo-3 AM-loaded J774 cells were pretreated with 1 μg/ml *Neurospora crassa* NADase. Ten min later, forkolin was added to the cells and [Ca^{2+}]$_i$ changes were measured using a confocal microscope. *E*, IgG increases Cx43 phosphorylation. J774 cells were treated with IgG complex for the indicated time. The cell lysates were immunoblotted with antibodies for Cx43 and β-actin. *F*, effect of H89 on FcγR stimulation-induced Cx43 phosphorylation. J774 cells were treated with IgG complex for 20 s in the presence of 0–1 μM H89. The cell lysates were immunoblotted with antibodies for Cx43 and β-actin. Each *line* represents mean $\pm$ S.E. of [Ca^{2+}]$_i$ (*A*, *B*, and *D*).

knockdown did not (Fig. 3*E*). We also found that extracellular cADPR induces [Ca^{2+}]$_i$ increase in HL 60 cells that do not express CD38 (data not shown). These data suggest that CD38 is not involved in the transport of extracellular cADPR in intact cells at least in Jurkat cells. Equilibrative and concentrative nucleotide transporters also have been suggested as a cADPR importer in intact 3T3 fibroblast and Hela cells (17). However, it is unclear whether nucleoside transporters are linked to CD38 signaling. It does not appear that Cx43 hemichannels are involved in all CD38/cADPR/Ca^{2+} signaling. T and B cells have no Cx43 but have a CD38/cADPR/

Ca^{2+} signaling system. Thus we cannot rule out that oligomeric CD38 or nucleoside transporter act as a cADPR importer in CD38/cADPR/Ca^{2+} signaling system in Cx43 non-expressing cells. We identified a new function of Cx43 hemichannels as a cADPR transporter. Our results suggest that Cx43 hemichannels are a linker of extracellular cADPR generation and its intracellular action.

It has been shown that a rise in intracellular Ca^{2+} concentration functions as a second messenger for phagocytosis although several studies have shown conflicting results (23–25). McNeil *et al.* (24) reported that aquorin-loaded adherent macrophages
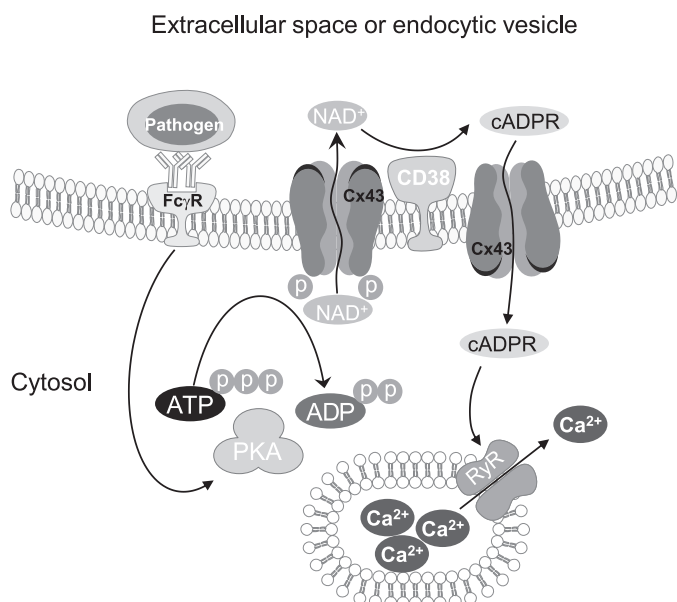
Extracellular space or endocytic vesicle

FIGURE 7. A model for FcγR stimulation-induced [Ca^{2+}]$_i$ increase via Cx43/CD38/cADPR signaling pathway. FcγR stimulation activates PKA, which causes Cx43 phosphorylation. Cx43 phosphorylation induces NAD$^+$ secretion. Extracellular NAD$^+$ is converted into cADPR, which is imported into cytosol via Cx43 and increases [Ca^{2+}]$_i$ via RYR.

elicited with thioglycolate broth injection did not show a rise in [Ca^{2+}]$_i$ during phagocytosis of IgG-coated red blood cells. In contrast, Di Virgilio *et al.* (23) found that the increase in [Ca^{2+}]$_i$ was variable in an adherent population of thioglycolate-elicited macrophages as assessed by fura-2 fluorescence. Kruskal and Maxfield (26) postulated that the undetectability of [Ca^{2+}]$_i$ might be due to an asynchronous event of phagocytosis where Ca^{2+} increases in different cells at different times have been averaged. Hishikawa *et al.* (27) solved this problem by using a digital video imaging system and demonstrated that initiation of phagocytosis was always preceded by an associated Ca^{2+} increase. Another unsolved issue is the identity of the second messenger involved in the Fcγ-mediated increase in [Ca^{2+}]$_i$. In neutrophils, monocytes, and mast cells, Fcγ-mediated increases in [Ca^{2+}]$_i$ have been found to be independent of inositol trisphosphate (IP$_3$) (28–30). However, in U937 cells, a more differentiated macrophage type cell, IP$_3$ is the second messenger for Fcγ-mediated increases in [Ca^{2+}]$_i$, indicating that the second messenger for Fcγ-mediated increases in [Ca^{2+}]$_i$ may vary according to the differentiation state of a cell (30). In this study we demonstrated that FcγR stimulation increases intracellular Ca^{2+} via CD38/Cx43/cADPR signaling pathway in macrophages.

FcγR stimulation, extracellular NAD$^+$ and cADPR-induced increase in [Ca^{2+}]$_i$ showed a peak instead of a long lasting property, indicating the tight regulation of cADPR influx. We found that A23187, a Ca^{2+} ionophore, blocks cADPR uptake in J774 cells (data not shown). The rapid decline of [Ca^{2+}]$_i$ after a rise could be mediated by rapid Cx 43 closing, which might be a negative feedback loop in regulation of [Ca^{2+}]$_i$. This is supported by the reports that Cx43 opening is negatively regulated by intracellular Ca^{2+} (31). In addition, Cx43 permeability is negatively regulated by PKC which is activated by the elevation of [Ca^{2+}]$_i$ (32–33). However, a PKC inhibitor did

not affect extracellular cADPR-induced [Ca^{2+}]$_i$ increase. Another signal besides PKC appears to be involved in [Ca^{2+}]$_i$-sensitive Cx43 hemichannel closing, which is needed for further studies.

Clustering of FcγR induces an increase in [Ca^{2+}]$_i$, thereby regulating FcγR-mediated phagocytosis. The second messenger of FcγR-stimulation induced increase in [Ca^{2+}]$_i$ is cADPR whose production and delivery to its action site is tightly regulated by the Cx43/CD38 system. Our result is the first evidence showing the regulation of FcγR-mediated phagocytosis by CD38/cADPR/Ca^{2+}. One of the phenotype of CD38 knock-out mice is the sensitivity to bacterial infection (34). Partida Sanchez *et al.* demonstrated that the susceptibility to bacterial infection is due to an inability of CD38-knock-out neutrophils to induce [Ca^{2+}]$_i$ release in response to a chemoattractant and migrate to the site of infection (34). According to our results, the inability of CD38-knock-out macrophages to induce FcγR-induced [Ca^{2+}]$_i$ release and the decrease of FcγR-mediated phagocytosis also contributes to the susceptibility to bacterial infection.

REFERENCES

1. Mészáros, L. G., Bak, J., and Chu, A. (1993) *Nature* **364,** 76–79
2. Lee, H. C., Galione, A., and Walseth, T. F. (1994) *Vitam. Horm.* **48,** 199–257
3. Schwarzmann, N., Kunerth, S., Weber, K., Mayr, G. W., and Guse, A. H. (2002) *J. Biol. Chem.* **277,** 50636–50642
4. Noguchi, N., Takasawa, S., Nata, K., Tohgo, A., Kato, I., Ikehata, F., Yonekura, H., and Okamoto, H. (1997) *J. Biol. Chem.* **272,** 3133–3136
5. Tang, W. X., Chen, Y. F., Zou, A. P., Campbell, W. B., and Li, P. L. (2002) *Am. J. Physiol. Heart Circ. Physiol.* **282,** H1304–1310
6. Galione, A., Lee, H. C., and Busa, W. B. (1991) *Science* **253,** 1143–1146
7. Shen, S. S., and Buck, W. R. (1993) *Dev. Biol.* **157,** 157–169
8. Han, M. K., Cho, Y. S., Kim, Y. S., Yim, C. Y., and Kim, U. H. (2000) *J. Biol. Chem.* **275,** 20799–20805
9. Funaro, A., Spagnoli, G. C., Ausiello, C. M., Alessio, M., Roggero, S., Delia, D., Zaccolo, M., and Malavasi, F. (1990) *J. Immunol.* **145,** 2390–2396
10. Rakovic, S., Galione, A., Ashamu, G. A., Potter, B. V., and Terrar, D. A. (1996) *Curr. Biol.* **6,** 989–996
11. Takasawa, S., Nata, K., Yonekura, H., and Okamoto, H. (1993) *Science* **259,** 370–373
12. Han, M. K., Kim, S. J., Park, Y. R., Shin, Y. M., Park, H. J., Park, K. J., Park, K. H., Kim, H. K., Jang, S. I., An, N. H., and Kim, U. H. (2002) *J. Biol. Chem.* **277,** 5315–5321
13. Malavasi, F., Deaglio, S., Funaro, A., Ferrero, E., Horenstein, A. L., Ortolan, E., Vaisitti, T., and Aydin, S. (2008) *Physiol. Rev.* **88,** 841–886
14. De Flora, A., Franco, L., Guida, L., Bruzzone, S., Usai, C., and Zocchi, E. (2000) *Chem. Immunol.* **75,** 79–98
15. Bruzzone, S., Guida, L., Zocchi, E., Franco, L., and De Flora, A. (2001) *FASEB J.* **15,** 10–12
16. Franco, L., Guida, L., Bruzzone, S., Zocchi, E., Usai, C., and De Flora, A. (1998) *FASEB J.* **12,** 1507–1520
17. Guida, L., Bruzzone, S., Sturla, L., Franco, L., Zocchi, E., and De Flora, A. (2002) *J. Biol. Chem.* **277,** 47097–47105
18. Zembala, M., and Asherson, G. L. (1970) *Immunology* **19,** 677–681
19. Kim, S. Y., Kim, S. J., Kim, B. J., Rah, S. Y., Chung, S. M., Im, M. J., and Kim, U. H. (2006) *Exp. Mol. Med.* **38,** 535–545
20. Tsien, R. Y., Pozzan, T., and Rink, T. J. (1982) *Nature* **295,** 68–71
21. Kim, U. H., Han, M. K., Park, B. H., Kim, H. R., and An, N. H. (1993) *Biochim. Biophys. Acta* **1178,** 121–126

22. Song, E. K., Lee, Y. R., Yu, H. N., Kim, U. H., Rah, S. Y., Park, K. H., Shim, I. K., Lee, S. J., Park, Y. M., Chung, W. G., Kim, J. S., and Han, M. K. (2008) *Biochem. Biophys. Res. Commun.* **367,** 156–161

23. Di Virgilio, F., Meyer, B. C., Greenberg, S., and Silverstein, S. C. (1988) *J. Cell Biol.* **106,** 657–666

24. McNeil, P. L., Swanson, J. A., Wright, S. D., Silverstein, S. C., and Taylor, D. L. (1986) *J. Cell Biol.* **102,** 1586–1592

25. Young, J. D., Ko, S. S., and Cohn, Z. A. (1984) *Proc. Natl. Acad. Sci. U.S.A.* **81,** 5430–5434

26. Kruskal, B. A., and Maxfield, F. R. (1987) *J. Cell Biol.* **105,** 2685–2693

27. Hishikawa, T., Cheung, J. Y., Yelamarty, R. V., and Knutson, D. W. (1991) *J. Cell Biol.* **115,** 59–66

28. Choi, O. H., Kim, J. H., and Kinet, J. P. (1996) *Nature* **380,** 634–636

29. Rosales, C., and Brown, E. J. (1992) *J. Biol. Chem.* **267,** 5265–5271

30. Melendez, A., Floto, R. A., Gillooly, D. J., Harnett, M. M., and Allen, J. M. (1998) *J. Biol. Chem.* **273,** 9393–9402

31. De Vuyst, E., Wang, N., Decrock, E., De Bock, M., Vinken, M., Van Moorhem, M., Lai, C., Culot, M., Rogiers, V., Cecchelli, R., Naus, C. C., Evans, W. H., and Leybaert, L. (2009) *Cell Calcium* **46,** 176–187

32. Bruzzone, S., Franco, L., Guida, L., Zocchi, E., Contini, P., Bisso, A., Usai, C., and De Flora, A. (2001) *J. Biol. Chem.* **276,** 48300–48308

33. Bao, X., Lee, S. C., Reuss, L., and Altenberg, G. A. (2007) *Proc. Nat'l Acad. Sci. U.S.A.* **104,** 4919–4924

34. Partida-Sánchez, S., Cockayne, D. A., Monard, S., Jacobson, E. L., Oppenheimer, N., Garvy, B., Kusser, K., Goodrich, S., Howard, M., Harmsen, A., Randall, T. D., and Lund, F. E. (2001) *Nat. Med.* **7,** 1209–1216